Article

Power Quality Assessment in a Real Microgrid-Statistical Assessment of Different Long-Term Working Conditions

Anna Ostrowska [1], Łukasz Michalec [1,*], Marek Skarupski [2], Michał Jasiński [1,*], Tomasz Sikorski [1], Paweł Kostyła [1], Robert Lis [1], Grzegorz Mudrak [3] and Tomasz Rodziewicz [3]

1   Faculty of Electrical Engineering, Wroclaw University of Science and Technology, 50-370 Wroclaw, Poland
2   Faculty of Pure and Applied Mathematics, Wrocław University of Science and Technology, 50-370 Wrocław, Poland
3   TAURON Dystrybucja S.A., 31-060 Kraków, Poland
*   Correspondence: lukasz.michalec@pwr.edu.pl (Ł.M.); michal.jasinski@pwr.edu.pl (M.J.); Tel.: +48-71-320-202 (M.J.)

Abstract: Power quality (PQ) becomes a more and more pressing issue for the operation stability of power systems with renewable energy sources. An important aspect of PQ monitoring of distribution networks is to compare the PQ indicators in different operating conditions. This paper evaluates the impact of a microgrid implementation in a real distribution network on power quality indicators at the point of common coupling in an LV network. The study includes a classical assessment of the long-term PQ parameters according to the EN 50160 standard, such as nominal frequency deviations, voltage RMS variations, voltage fluctuations (represented by long-term flicker severity), voltage unbalance and total harmonic distortion. The PQ evaluation is extended in statistical assessment based on cluster analysis. The case study contains 5 weeks of power quality observation results obtained at the assessment point in two different working conditions of the distribution system: before and after implementing the microgrid. The study allows establishing general conclusions regarding a microgrid interconnection in order not to exceed power quality limits and considering the influence of photovoltaic generation on power quality parameters.

Keywords: distributed generation; energy storage island mode; microgrid; power quality; renewable energy resources; long-term assessment

1. Introduction

The energy sector is undergoing an extreme transformation from the centralized energy concept to a distributed energy concept. The new concept is flexible and local, and the leading role in energy generation is played by renewable energy sources (RES) [1,2]. Common examples of RES include solar photovoltaic (PV) units, wind generators, micro-turbines and energy storage systems [3,4]. The prominent development of RES on a large scale has been observed in recent years in many countries, including Poland. In particular, the generation of electricity in photovoltaic power plants, wind farms and agricultural biogas plants has the greatest development potential in this country [5,6]. The accepted target of a 15% share of energy generated from renewable energy sources in final energy consumption, and the need to reduce environmental pollution, are the main causes of implementing distributed generation (DG) in Poland to achieve socio-economic benefits for sustainable development [7,8]. The popularity of DG, based on renewable energy sources, modifies the traditional structure of the electric utility grid and opens the way for self-sustainable entities called microgrids [9,10]. Subsequently, the power industry model will be transformed into a system based on local self-balancing energy areas and smart grids [11,12]. It introduces the need for analyzing and simulating an increasing amount of data. Distribution system operators can use this data to take preventive steps to avoid deterioration and improve the power quality (PQ) level [13–15]. Thus, the tools to support

microgrid systems and power quality improvement have become desirable. There have been several developments in this field, such as the application of artificial intelligence based on the Icos control algorithm to improve the intelligence of grid-integrated power systems [16] or the use of digital approaches to implementing control strategies [17].

The main contribution of the paper is to conduct the statistical power quality assessment and comparative analysis of different long-term working conditions in a real microgrid.

2. Literature Review

Power systems are facing challenges to provide efficient and reliable electrical energy to customers, associated with increasing power demand, while primary energy resources are being limited. Thus, the necessity of power generation from distributed energy sources is considerable. However, it brings challenges for the utility and system operators, such as the intermittency of power generation, as well as identifying and analyzing power quality problems [18,19]. This section provides an overview of microgrid architectures and regulatory control techniques. The second part of the Section 2 focuses on current knowledge about the evaluation of the power quality and reliability of distributed generation in MG structures.

2.1. Microgrid Architecture

The traditional power distribution structure (centralized generation) is formed by large-capacity power plants using fossil fuels (coal power plants, nuclear power plants, etc.) usually placed far from the consumers (electric demand) [20]. The concept of the MG has been developed to be a self-sustaining cluster (decentralized generation) consisting of small-power-capacity distributed generators (DGs), energy storage systems (ESS) and local electricity demand (electrical loads), with the ability to operate connected to the utility grid or in islanded mode [21–23]. Microgrids are connected to the main grid through a point of common coupling (PCC) (Figure 1) and can be subject to high variations in terms of voltage and frequency, which challenge their stability. Thus, in microgrids, the energy management system, which controls the charging and discharging of energy storage equipment, is essential for the optimal use of distributed energy sources in an intelligent, safe, reliable and coordinated manner. In this way, it is ensured that electric energy meets the load demand in different periods [23].
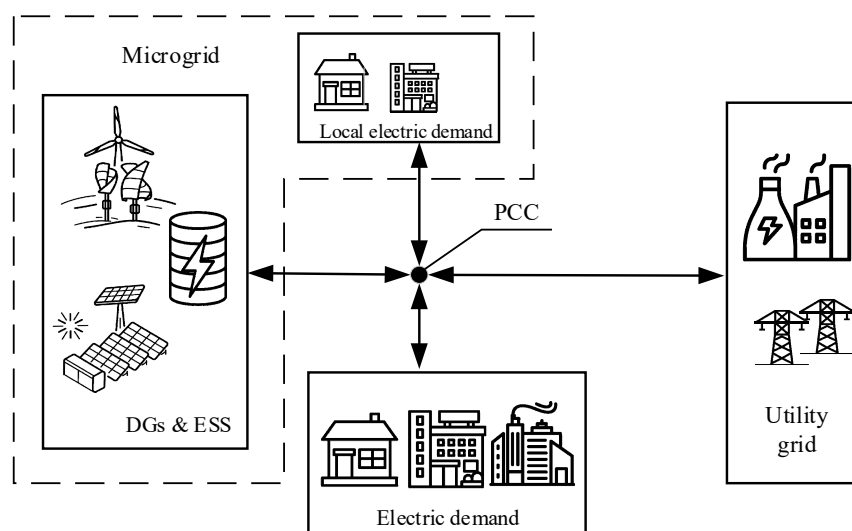

Figure 1. Simplified diagram of a distribution network with a microgrid (own elaboration based on data from [24]).

Several factors, such as public awareness of climate change, rising fuel costs and blending digital technologies with power system operation, have led to the transition from

the conventional grid to the smart grid. Enhancing smart grids with MGs is a prominent opportunity but also brings challenges. Control of generation, weather forecasting, data transmission and monitoring techniques are considered as smart functions in MGs [25,26]. In addition, various architectures of MGs are available and many more are still being developed [27]. The architecture of an MG depends on several factors such as the availability of renewable resources, geographical location, load demand, etc. [28]. An AC microgrid is the primary microgrid architecture for powering distribution networks. It can be directly connected to the existing distribution networks without or with minimum energy transformation [29,30]. However, the concept of a DC microgrid has arisen as the majority of DERs generate DC power and the use of DC loads have increased in recent years [31,32]. The main advantages of the DC microgrid are high efficiency, the fact that it requires no reactive power, and eliminates the need for AC/DC or DC/AC switching stages [33]. However, since the existing distribution networks and most loads are operated at AC power, the AC microgrids are still dominant [34]. Thus, by merging the DC microgrid with the AC microgrid through a bidirectional interlinking converter (ILC), the advantages of both microgrids are extracted, and this combined architecture has gained popularity in recent years. The concept of combining DC and AC architectures is known as hybrid AC/DC microgrids [35,36]. Apart from the type of architecture and mode of operation, MGs are also classified concerning the type of regulatory control and application (Figure 2).
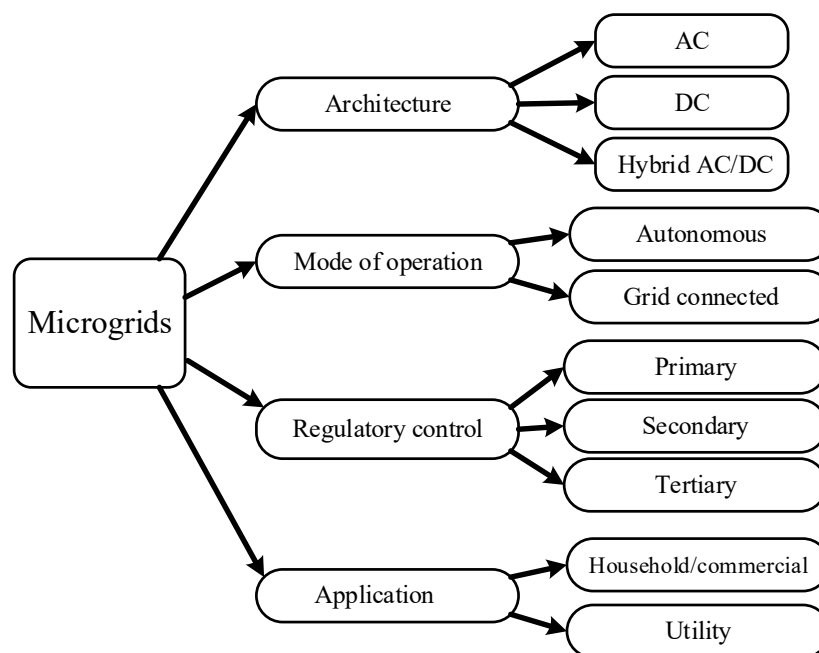
Figure 2. Classification of microgrids (own elaboration based on data from [13]).

There are three main types of microgrid regulatory control techniques: primary, secondary, and tertiary. The primary control provides a stable voltage/frequency and does not require a communication link as it operates locally. The secondary control method improves the power quality and energy management of microgrids after the local control actions. In a decentralized case of secondary control, a whole microgrid is supervised utilizing data that are collected from each distributed energy resource separately. In a centralized case, a central controller is applied and a microgrid network and loads provide up-to-date information that is used to make the best possible control decisions. The last regulatory control method becomes effective after the second control level and improves power quality by coordinating energy between various microgrids and the utility grid, providing its users with financial and technical advantages such as increased grid reliability and lower energy production costs [34,37].

Achieving these benefits is challenging, and the cost of microgrid implementation can be high, as a microgrid requires additional investment in supporting technologies and temporary modifications. The techno-economic analysis of a grid-connected microgrid deployment, which consists of a photovoltaic (PV) and energy storage system, show that further encouraging actions from utilities or governments are required to make microgrids economically sustainable [38–40].

2.2. Power Quality in Microgrids

With the continuous development of new energy power generation technology, the access capacity of distributed power sources has been continuously increasing [41]. This brings problems to the power system planning and relay protection of the power grid, and also impacts the power quality of the distribution networks. Low power quality can affect the normal operation and lifetime of the equipment to a certain extent. It also may lead to economic losses and large-scale power outages in serious cases [42]. The structure of the microgrid, which is generally built at the final part of the distribution network, is the main form of increasing penetration of distributed generation and one of the reasonable methods of connecting aggregated low-power sources to the traditional power system [40]. However, connecting renewable energy resources (RES) to the power system creates decentralized generation, which is associated with [43]:

- bidirectional energy flow;
- access to a large number of power electronic devices (inverters, controllers);
- the stochastic nature of RES generation.

Compared with centralized generation, the structure of the microgrid is different and susceptible to these factors. Thus, the power quality problem becomes more complicated for decentralized generation [44]. The power quality of the microgrid is simultaneously affected by the load side, the distributed generation side and the grid side, which makes it more difficult to analyze and control [45]. Consequently, an increasing number of researchers are paying attention to the power quality issues of microgrids. Usually, undesirable disturbances may appear in the form of long-term voltage variations, i.e., voltage fluctuations, as well as deviations in the nominal frequency and voltage RMS values. Additionally, several studies have been conducted assessing the impact of DG on other power quality indices, such as voltage unbalance [46–48] and harmonics [49–57].

Power quality problems, such as voltage fluctuations and frequency deviations, are caused by the intermittent nature of DGs that are present in inverter-based microgrid design [58–60]. However, for the microgrids operating in grid mode, the primary and secondary regulatory control techniques (described in Section 2.1) help stabilize voltage and frequency profiles and keep them within a relatively small range of deviations from the nominal value. In the article [61], the voltage and frequency stability problems were experimentally analyzed and advanced mitigation techniques were proposed. The research was performed at the Maui Smart Grid project in Hawaii. The microgrid consisted of two MW of distributed PV generation. From the conditions when the distributed voltage decreases beyond the nominal value, the smart PV inverters using the volt-watt control method (described in detail in the paper) can control the voltage within the nominal range. It is emphasized that over-power generation can cause the over-frequency problem of a power system. Depending on the frequency set points, grid over-frequency can be also regulated by the smart PV inverter using the over-frequency control method, which is based on the frequency–watt curve.

Due to the existence of a large number of single-phase equipment in microgrids, the three-phase balanced structure of the distribution network can be seriously damaged [48]. Additionally, the power grid influence brings the problem of a three-phase voltage imbalance into the microgrid [48]. The authors of the paper [46] assess the impact of photovoltaic distributed generation (PVDG) on the power quality indices (PQI) of distribution networks using three techniques: time series analysis, quasi-sequential Monte Carlo simulation and radial power flow based on the phase coordinates method. The experimental results in

a feeder with 1595 nodes presented that the voltage unbalance index undergoes large variations when the photovoltaic power plant is connected to distribution networks. The effect of a PVDG on the PQI is not continuous, while a solar generation plant can produce energy only during periods of sunshine. Thus, analyzing the PQI, it is necessary to forecast weather condition variations during a certain period.

In microgrids with PVDG, most negative impacts on the PQ level emerge from current distortion [62]. There is a large number of pieces of distributed power generation equipment and some user loads which are connected to the PCC through one- or multi-level conversion using power electronic converters. Thus, the prominent harmonic problem of the microgrid caused by a higher proportion of non-linear loads exists in a wide-band frequency domain [56]. PV inverters are regarded as harmonic-producing devices [63]. The sinusoidal pulse width modulation (SPWM) inverter circuit is usually used when the microgrid is performing AC/DC conversion [49]. To make the output waveform close to the ideal sine wave, the carrier frequency is in the range of 1–15 kHz. Thus, the harmonics in the system not only contain the low-order harmonics of the power frequency integral times but also contain the high-frequency harmonics (supraharmonics). At the same time, the connection of nonlinear components on the load side also gives rise to harmonic problems. In the article [62], THD analysis was conducted at different levels of PV penetration along with linear and non-linear loads connected to the microgrid system. The THD was found at around 4% at a higher level of PV penetration level along with linear load, whereas at a minimum level of PV penetration with a connection of non-linear load, the THD level was found to be 5.06%.

The authors of the article [55] conducted field measurements to characterize the harmonic emission behavior of the microgrid, consisting of a 100 kW photovoltaic installation including 16 single-phase inverters. The measured harmonic currents were compared with emission values provided by the manufacturer as well as emission limits specified in standards. The analysis of the PV installation shows that the third, fifth and seventh harmonics are the dominating current harmonic components, with about 3.9 A total harmonic current (THC), which corresponds to about 2.6% total demand distortion (TDD). The harmonic currents of the whole PV installation meet the limits of the IEEE standard 519-2014 [64]. Even if PV inverters all belong to the same type, a certain deviation in the harmonic current between the different inverters can be observed.

In active distribution networks [65], it is a challenging task for the utility and system operators to identify and analyze the power quality (PQ) disturbance and its cause. Thus, monitoring the overall quality of the power in distribution networks has become a significant concern. An appropriate measure and analysis of electromagnetic disturbances in networks show both the microgrid contribution to PQ deterioration and the influence of the utility grid perturbations on the performance parameters of the microgrid.

The power quality problems of microgrid systems cannot fully be reflected through a single power quality standard. Thus, power quality evaluation to establish a reasonable control method is the premise to ensure the stable operation of a microgrid, and it can provide a reference for better power quality management.

3. Methodology and Research Object

This article presents a case study of analyzing the real MV/LV distribution network in different working conditions that operates in Poland. The case study of PQ analysis was planned by considering the network before and after the implementation of the microgrid. The structure of the microgrid includes two sections. In Section 3.1, there is a photovoltaic power plant with a combined capacity of 189 kW. Section 3.2 consists of photovoltaic micro-installations with a combined capacity of 45.5 kWp and the total load capacity of 1535.7 kW. To conduct the measurements, a class A PQ analyzer (Fluke 1760) and its associated equipment were used. The indicated database consists of parameters, which are considered in the classical PQ assessment in accordance with the standard EN 50160:2015 [66].

The investigation was based on measurements that were obtained at the assessment points:

- before implementation of the microgrid into the system. The duration of the measurements was from 01 August 2021 to 05 September 2021;
- after implementing the microgrid into the system (synchronous operation of the microgrid and the system). The duration of the measurements was from 7 February 2022 to 14 March 2022;
- For the indicated measurement point and periods, the PQ assessment was realized using classical 10 min aggregated values of PQ parameters, and for the voltage changes and total harmonic distortion, the 200-ms values of local maximum and minimum were added. However, the obtained data can be also implemented for the comparison of microgrid nodes in terms of power quality using the global power quality index (GPQI) [67], but this issue is outside the scope of this paper. The research applied the rule of flagging and excluding events (dips, short and long interruptions) from the long-term assessment of aggregated values in accordance with the flagging concept of the standard IEC 61000-4-30 [68].

The statistical methods used in the paper were based on the Wilcoxon rank-sum test. The Wilcoxon rank-sum test is a nonparametric test that is based on the order of the observations from the two samples. Test statistic W is the sum of the ranks for observations from one of the samples. To obtain the *p*-value corresponding to the rank-sum test statistic W, we considered how rank-sums behave under the null hypothesis (shift parameters are equal), and how they behave under the alternative two-sided hypothesis (shift parameters are not equal). The *p*-value is the doubled probability of falling into the tail of the distribution closest to W. All calculations were made in R software. The tables for the Wilcoxon rank-sum test and tables for *p*-values are given in R.

3.1. Power Quality Limits

The assessment of power quality generally is based on voltage profile analysis. The most crucial power quality parameters are frequency variations, voltage magnitude variation, voltage fluctuation (flicker severity), voltage unbalance (asymmetry), voltage harmonics and rapid voltage changes (voltage dips and swells, transient overvoltages, voltage interruptions).

The classical power quality assessment is based on the analysis of the PQ level separately for all PQ parameters shown in Figure 3. In this paper, the PQ analysis concerns the long-term variations, i.e., frequency (f), voltage changes (U), voltage fluctuations, represented by long-term flicker severity (P_{lt}), voltage unbalance (k_{u2}) and voltage harmonics (THDu).

Power quality assessment includes 10 min aggregation intervals and the obligation to consider 100% of measured data taken for the assessment of voltage variation in a low voltage (LV) supply terminal. The assessment is based on the permissible limits defined in the standard EN 50160:2015 [66].

Permissible levels of the PQ parameters for a low-voltage network are presented in Table 1.

The data collection was performed with the use of a class A (in accordance with standard EN 61000-4-30 [68]) Fluke 1760 power quality analyzer, provided by the Faculty of Electrical Engineering, Wroclaw University of Science and Technology.

3.2. Research Object

The described case study of the microgrid was based on the fragment of the distribution network in Poland (presented in Figure 4), supplied from main power stations 110/20/6 kV. Two network circuits flow into the transformer's busbars: Section 1, generation (RES, battery energy storage); and Section 2, receiving generation (residential houses, commercial premises, prosumer photovoltaic micro-installations). A photovoltaic installation with a total installed power of 189 kWp and battery energy storage with a capacity of

200 kW (250 kWh) was connected to the generation section. The receiving section consisted of individual recipients included in 8 main cable lines, with a maximum length of 820 km each. The installed load power was 1535.7 kW. In addition, some PCC were expanded to include prosumer photovoltaic sources. The installed power in the PV installations in Section 2 was 45.5 kWp. The tested part of the network was covered by the Microgrid Management System, responsible for controlling the system in the event of a failure.

Table 1. Requirements regarding power quality in the low-voltage grid according to EN 50160 standard [66].

Parameter	Symbol	Limit
Power frequency	f	$\pm 1\%$ ($49.5 \div 50.5$) Hz for 99.5% of the measurement data set
Supply voltage	U	$\pm 10\%$ U_{ref} for 99% of the measurement data set
		$-15\%/+10\%$ U_{ref} for 100% of measurement data set
Flicker severity	P_{lt}	1.0 for 95% of the measurement data set
Voltage unbalance	k_{u2}	2% for 95% of the measurement data set
Harmonics	THDu	8% for 95% of the measurement data set
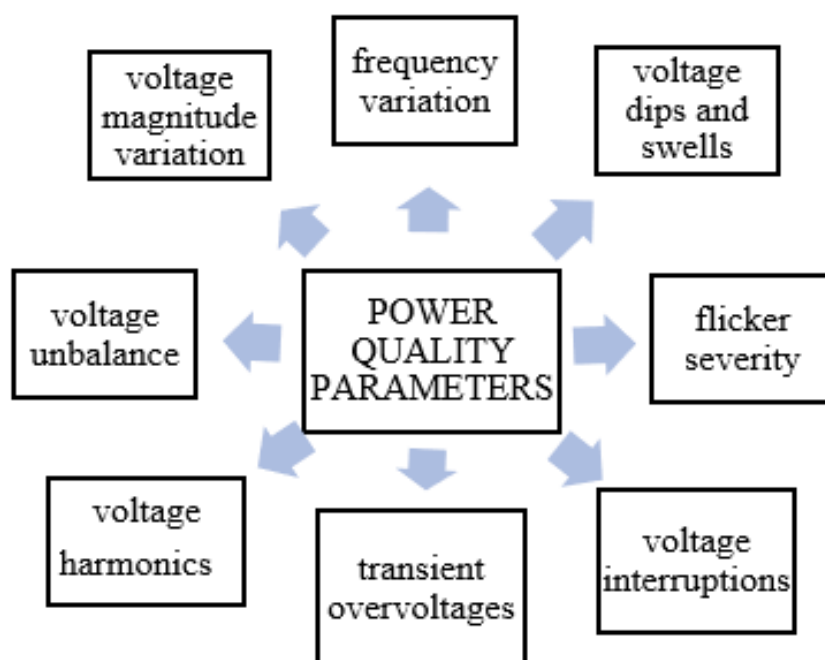
Figure 3. Power quality parameters [66].

The aggregation time of selected classical PQ parameters such as frequency, RMS level, flicker severity, unbalance, and harmonics PQ parameters was typically 10 min and the flagged data were extracted. Additionally, the data was extended by including parameters of an envelope of voltage deviation created by the maximum and minimum of 200-ms RMS values within 10 min.

In the analysis, the time when voltage events occurred was excluded. The event data exclusion was based on the flagging concept of standard IEC 61000-4-30 [68].
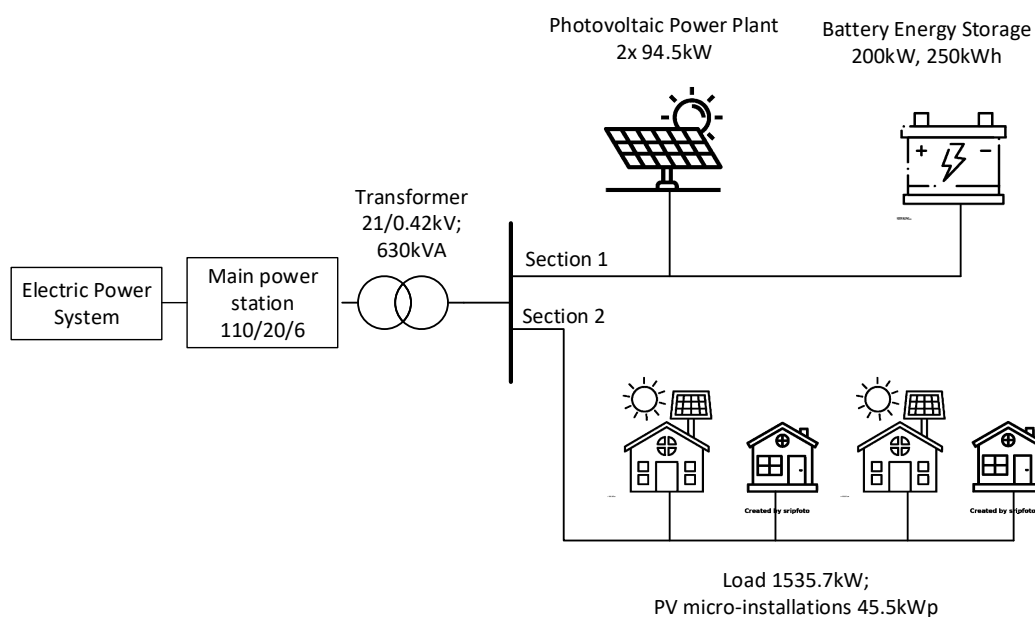
Figure 4. Diagram of the tested network.

4. Results

The obtained measurements were subjected to two types of analysis. First, each of the periods before and after the installation of the photovoltaic power plant was subjected to the classical methods of power quality analysis. It was assessed whether the parameters characterizing the structure met the requirements of EN 50160:2015 [66]. Next, a comparative analysis between the periods before and after the PV power plant implementation was conducted for each of the tested quality parameters. From the dataset, the basic parameters were calculated, such as minimum, maximum, mean, median, IQR and standard deviation. Together with the estimator of the probability distribution function, they were presented graphically on violin plots. The distribution of the results is unknown, as are the parameters of this distribution. In order to verify the hypothesis of normal distribution, the Anderson–Darling test was performed. In most cases, the hypothesis of the normality of the distribution of results was rejected. The result of this procedure is the selection of tests for the equality of the shift parameter between individual classes. For this purpose, the Wilcoxon rank-sum test with continuity correction was performed. In both tests, the significance level was $\alpha = 0.05$. The calculations were performed in R software.

To make a visualization of the data, we presented the violin plots for each cluster. Inside each of them, there is a box plot containing summary statistics such as median, both quartiles, IQR and outliers. Violin plots show also a kernel density plot, which shows peaks in the data. The shape of the distribution indicates the concentration of the measurement around the median.

4.1. Power Quality Analysis

Each of the plots, collected in Figure 5, shows changes in individual PQ parameters (left *Y*-axis) versus time (*X*-axis). Additionally, there are also station load value changes (right *Y*-axis, auxiliary) in relation to time. Voltage and THDu plots have been compiled for each phase separately and named sequentially as L1, L2, and L3.

The first period was characterized as a condition of the distribution network before microgrid implementation and power generation from renewable energy sources inside the network origin exclusively from prosumer PV installations. After the microgrid implementation (Period 2), an additional renewable energy source was applied to the network: a photovoltaic power plant. The aim of the analysis was to present the potential changes in the levels of power quality parameters in the newly created microgrid structure compared

to the previous one. For this purpose, 5-week observation periods were selected: before the creation of the microgrid, i.e., from 1 August 2021 to 5 September 2021, and after the creation of the microgrid, i.e., from 7 February 2022 to 14 March 2022.
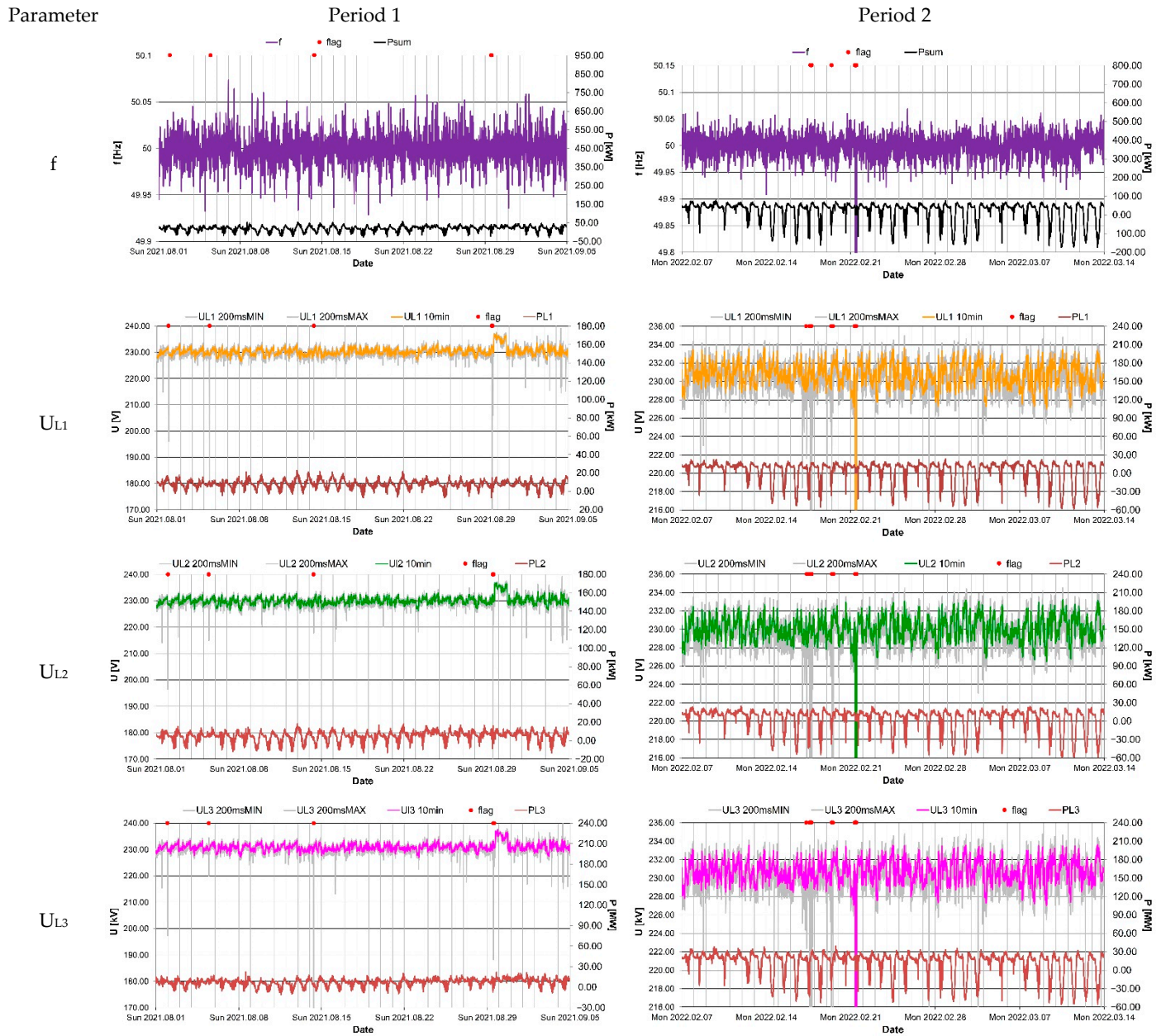
Figure 5. *Cont*.
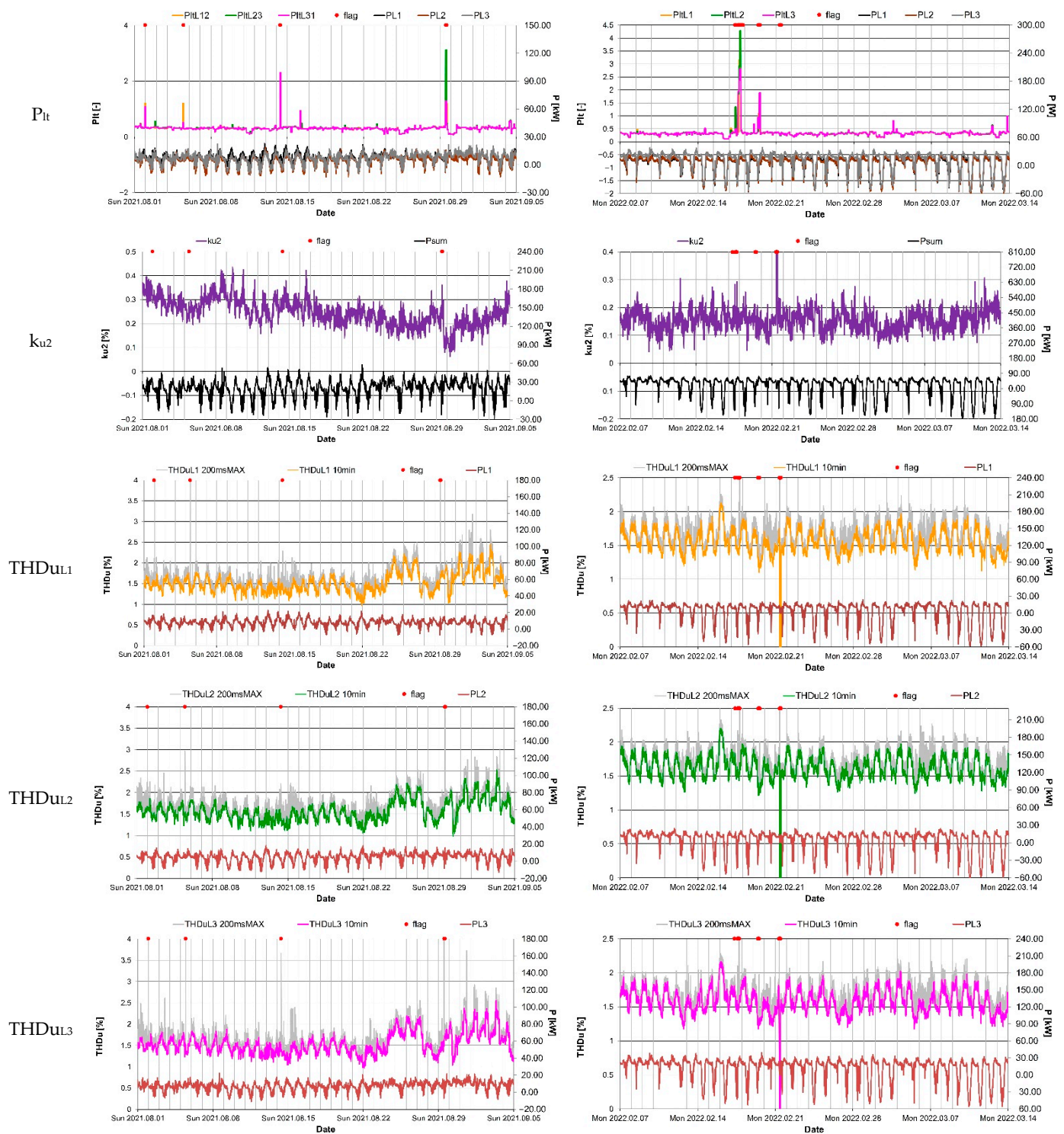
Figure 5. The course of the variability of the parameter in the tested measuring point for Period 1 (before the microgrid implementation) and Period 2 (after the microgrid implementation).

In the case of the analysis of the variability of the indicated parameters at the tested measuring point, before the creation of the microgrid (synchronous operation of the microgrid and the system) for the entire period, even taking into account the extreme values of 200 ms, it should be observed that the individual parameters were not subject to a significant absolute change, i.e.,

- The frequency changes were within a range not exceeding 0.072 Hz;

- The voltage values were fluctuating within a variation range not exceeding 7.33 V;
- Voltage fluctuations were represented by P_{lt} within 0.19;
- Asymmetry changes within the range were not exceeding 0.12%;
- The content of harmonics represented by THDu were in the range of 0.8%.

In the case of the analysis of the variability of the indicated parameters at the tested measuring point, after the creation of the microgrid (synchronous operation of the microgrid and the system) for the entire period, even taking into account the extreme values of 200 ms, it should be observed that the individual parameters were not subject to a significant absolute change, i.e.,

- The frequency changes were within a range not exceeding 0.091 Hz;
- The voltage values fluctuated within a variation range not exceeding 3.69 V;
- Voltage fluctuations were represented by P_{lt} within 0.11;
- Asymmetry changes within the range were not exceeding 0.12%;
- The content of harmonics represented by THDu were in the range of 0.8%.

Table 2 shows that despite the greater generation resources available after the implementation of the microgrid, the network achieved requirements for a power quality parameter according to EN 50160:2015 standards [66].

Table 2. Collective statement of achievement or non-achievement of the requirements for a power quality parameter according to EN 50160:2015 standards [66].

Parameter	Symbol	Period 1	Period 2
Power frequency	f	✔	✔
Supply voltage	U	✔	✔
Flicker severity	P_{lt}	✔	✔
Voltage unbalance	k_{u2}	✔	✔
Harmonics h2–h40	$THDu_U$	✔	✔

4.2. Comparative Assessment

In the next step, as part of the extended assessment, both indicated five-week periods were divided into different clusters depending on the operating status of the tested part of the network shown in Figure 6. The first division was made in relation to the time of day—day and night, assuming the day was between 6 a.m.–7 p.m. and the night the remaining hours. The indicated hours were related to the time of sunrise and sunset in the studied periods and averaged. In addition, the time of the day was divided into two criteria due to the nature of the tested part of the network, i.e.,

- When the local generation fully meets local demand (cluster 3);
- When the local generation does not meet local demand (clusters 1 and 2).

During the night, there were no data on which the local generation covered the local demand.

Hence, for the comparative assessment, three periods were distinguished, referred to as "clusters" (groups of data with common features—in this case, the time of day and the generation level in relation to the demand in the examined fragment of the power grid):

- Cluster 1—night represented by 2310 10 min data (approximately 46% of the measurement time);
- Cluster 2—day without full coverage of local demand represented by 1737 10 min data (approximately 35% of the measurement time);

- Cluster 3—day with full coverage of local demand represented by 971 10 min data (approximately 19% of the measurement time).
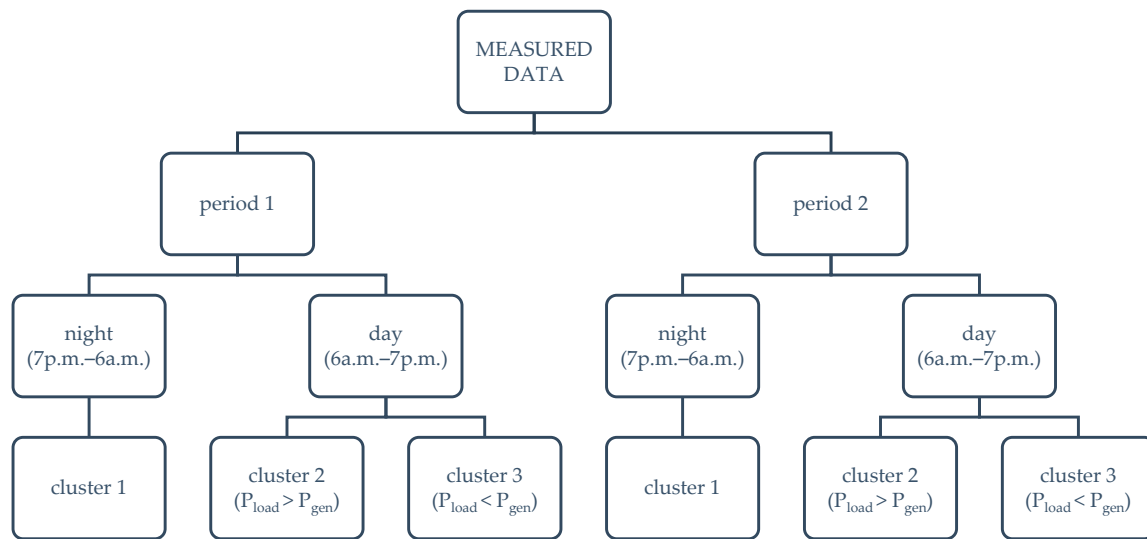
Figure 6. Diagram of the division of the measured data into individual periods and clusters.

4.2.1. Frequency

Statistical tests were performed for the frequency. The data were statistically analyzed on the basis of the following values: minimum, maximum, mean, median, standard deviation, first and third quantiles (Table 3), confirming that the parameters were within the required range. The Wilcoxon rank-sum test was carried out with continuity correction (Table 4) on the significance level $\alpha = 0.05$. Null hypothesis: true location shift between the same clusters in different periods is 0 (red color in table). Alternative hypothesis: true location shift is not equal to 0 (color in table). Data distribution is shown in the violin plots for both periods (Figure 7).

Table 3. Descriptive statistics of the frequency at the tested measuring point.

Parameter	Period 1			Period 2		
	Cluster 1	Cluster 2	Cluster 3	Cluster 1	Cluster 2	Cluster 3
Min	49.93	49.95	49.96	49.91	49.93	49.93
1st Qu	49.99	49.99	49.96	49.99	49.99	49.99
Median	50.00	50.00	50.00	50.00	50.00	50.00
Mean	50.00	50.00	50.00	50.00	50.00	50.00
3rd Qu	50.01	50.01	50.01	50.01	50.01	50.01
Max	50.07	50.06	50.06	50.06	50.07	50.04
St. Dev.	0.016	0.013	0.013	0.018	0.018	0.017

Table 4. Wilcoxon rank-sum test of the shift parameter for frequency ($\alpha = 0.05$).

Clusters	1	2	3
W=	2,525,096	1,800,456	240,385
p-value	0.001419	0.07374	0.0004081

Data marked in red: the null hypothesis is true, which means values do not change between periods.
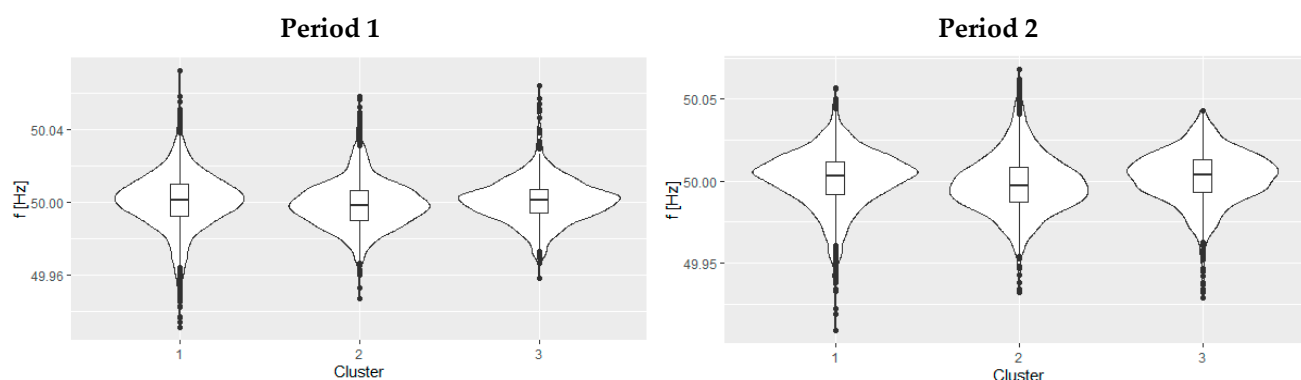
**Figure 7.** Violin plots of frequency comparing clusters for Period 1 and Period 2.

The statistical tests and test hypotheses show that the network frequency does not change (red, Table 4) between Periods 1 and 2 for Clusters 1 (night) and 3 (generation covers demand). The frequency varies between periods only for Cluster 2 (generation with MG does not cover demand).

The test confirmed that the frequency did not change due to the connection of the photovoltaic installation.

4.2.2. Voltage

Statistical tests were performed for the voltage. The data were statistically analyzed for each phase on the basis of the following values: minimum, maximum, mean, median, standard deviation, first and third quantiles (Tables 5–7), confirming that the parameters were within the required range. The Anderson–Darling normality test was carried out (Table 8). The Wilcoxon rank-sum test was carried out with continuity correction for each phase (Table 9) on the significance level $\alpha = 0.05$. Null hypothesis: true location shift between the same clusters in different periods is 0 (red color in table). Alternative hypothesis: true location shift is not equal to 0 (black color in table). Data distribution is shown in the violin plots (Figure 8) and box plots (Figure 9) for both periods. Both tests were performed on significance level $\alpha = 0.05$.

Table 5. Descriptive statistics of the voltage in phase L1 at the tested measuring point.

Parameter	Period 1			Period 2		
	Cluster 1	Cluster 2	Cluster 3	Cluster 1	Cluster 2	Cluster 3
Min	226.4	227.9	228.0	227.0	228.3	229.0
1st Qu	229.1	229.8	229.7	229.5	230.2	231.0
Median	229.7	230.6	230.3	230.2	230.9	231.6
Mean	229.8	230.5	230.3	230.3	230.9	231.6
3rd Qu	230.6	231.2	231.0	231.1	231.6	232.2
Max	233.5	234.2	233.2	233.7	233.4	233.6
St. Dev.	1.20	0.97	0.96	1.22	0.96	0.96

The Anderson–Darling test indicated a discrepancy from the normal distribution for Cluster 3 in phases L1 and L2 (black color, Table 8). For the remaining variants, the sets converged to the normal distribution. The distribution of the data is shown in Figure 8.

The statistical tests and test hypotheses show that the network voltage does not change (red, Table 9) between Periods 1 and 2 for Cluster 1 (night), phase L3, and Cluster 2 (generation with MG does not cover demand) phase L2, L3. The voltage varied between periods for Cluster 3 (generation cover demand) for all phases and for the rest of the phase in Cluster 1 and Cluster 3. For Cluster 3, the voltage in Period 2 increased, which was

caused by the increase in the share of the PV source in the system. The results of the Wilcoxon rank-sum test are shown in Figure 9.

Table 6. Descriptive statistics of the voltage in phase L2 at the tested measuring point.

Parameter	Period 1			Period 2		
	Cluster 1	Cluster 2	Cluster 3	Cluster 1	Cluster 2	Cluster 3
Min	226.2	227.6	227.9	226.4	227.9	228.4
1st Qu	228.7	229.6	229.4	228.9	229.5	230.3
Median	229.4	230.3	230.1	229.5	230.2	231.0
Mean	229.5	230.3	230.2	229.6	230.2	231.0
3rd Qu	230.2	231.0	230.8	230.3	230.9	231.7
Max	233.0	234.0	233.0	232.9	232.5	233.2
St. Dev.	1.21	0.96	0.94	1.18	0.95	1.01

Table 7. Descriptive statistics of the voltage in phase L3 at the tested measuring point.

Parameter	Period 1			Period 2		
	Cluster 1	Cluster 2	Cluster 3	Cluster 1	Cluster 2	Cluster 3
Min	226.9	228.6	228.7	227.0	228.4	229.2
1st Qu	229.6	230.4	230.2	229.5	230.1	230.9
Median	230.2	231.1	230.9	230.1	230.8	231.6
Mean	230.3	231.1	230.9	230.2	230.8	231.6
3rd Qu	231.0	231.8	231.5	230.9	231.6	231.2
Max	233.7	234.5	233.7	233.3	233.1	233.6
St. Dev.	1.19	0.93	0.96	1.18	0.93	0.97

Table 8. Anderson–Darling normality test of the voltage ($\alpha = 0.05$) in each phase.

Phase	Period	I			II		
	Cluster	1	2	3	1	2	3
L1	A=	10.495	1.6372	0.4493	3.8034	5.8403	2.0735
	p-value	<2.2×10^{-16}	0.0003332	0.2762	1.76×10^{-09}	2.243×10^{-14}	2.83×10^{-05}
L2	A=	10.899	1.37	0.70164	6.3382	5.0331	1.2789
	p-value	<2.2×10^{-16}	0.00151	0.0667	1.48×10^{-15}	1.915×10^{-12}	0.00252
L3	A=	12.048	1.7583	0.85627	5.8126	5.1961	1.637
	p-value	<2.2×10^{-16}	0.000168	0.02766	2.622×10^{-14}	7.787×10^{-13}	0.000332

Data marked in red: the null hypothesis is true, which means values do not change between periods.

Table 9. Wilcoxon rank-sum test of the shift parameter for voltage ($\alpha = 0.05$) in each phase.

Phase	Clusters	1	2	3
L1	W=	2,075,186	1,394,365	100,515
	p-value	<2.2×10^{-16}	<2.2×10^{-16}	<2.2×10^{-16}
L2	W=	2,459,191	1,825,554	146,966
	p-value	1.715×10^{-06}	0.9946	<2.2×10^{-16}
L3	W=	2,807,853	2,019,790	166,338
	p-value	0.9988	1	<2.2×10^{-16}

Data marked in red: the null hypothesis is true, which means values do not change between periods.
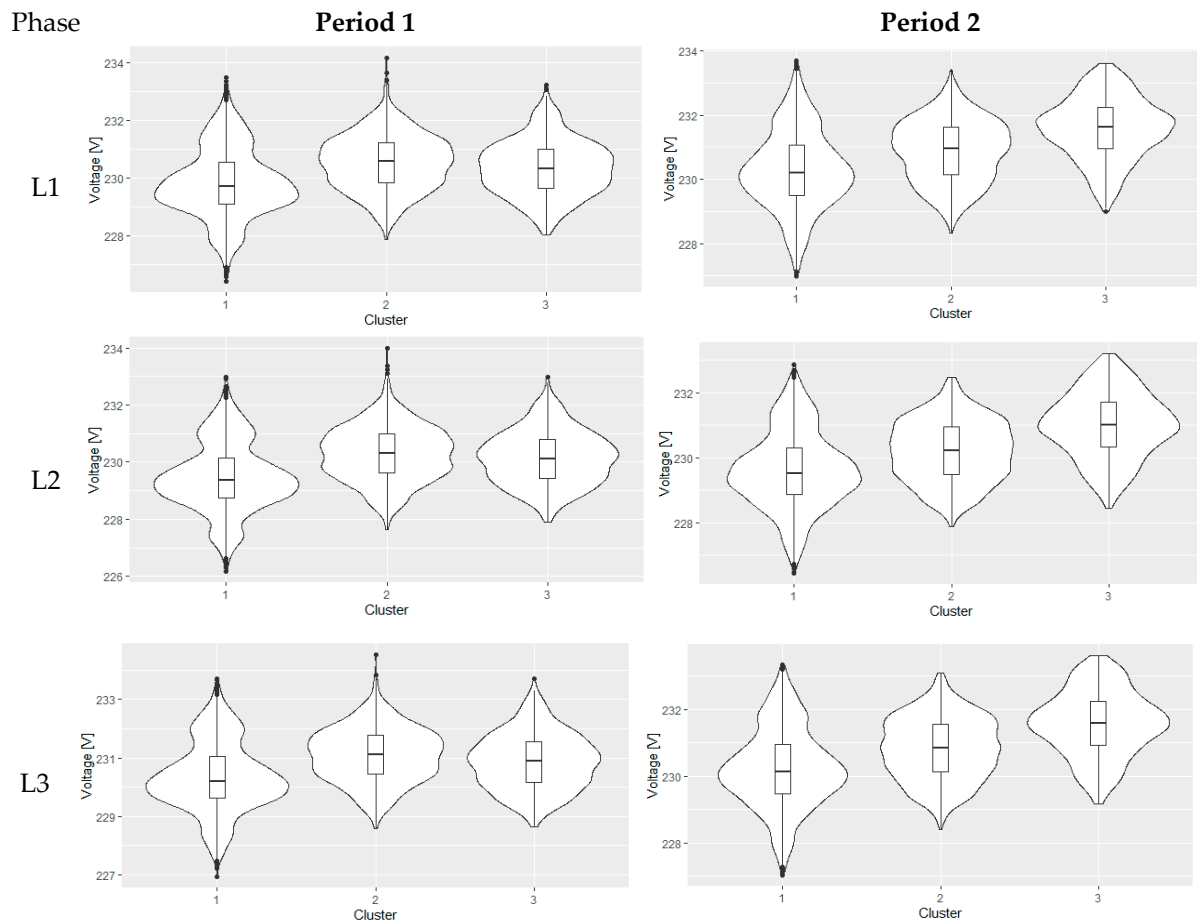
Figure 8. Violin plots of voltage comparing clusters for Period 1 and Period 2 in each phase.
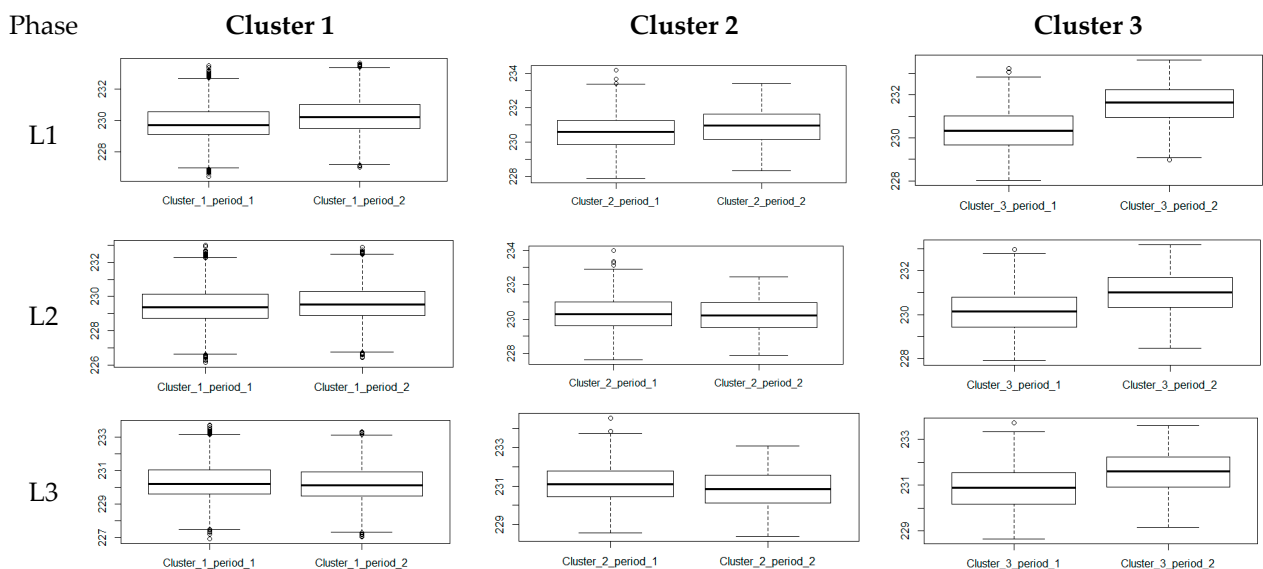
Figure 9. Box plots of voltage comparing periods for individual clusters in each phase.

4.2.3. Flickers

Statistical tests were performed for the power-line flickers (P_{lt}). The data were statistically analyzed for each phase on the basis of the following values: minimum, maximum, mean, median, standard deviation, first and third quantiles (Tables 10–12), confirming that the parameters were within the required range. The Wilcoxon rank-sum test was carried

out with continuity correction for each phase (Table 9) on the significance level $\alpha = 0.05$. Null hypothesis: true location shift between the same clusters in different periods is 0 (red color in table). Alternative hypothesis: true location shift is not equal to 0 (black color in table). Data distribution is shown in the violin plots (Figure 10) for both periods.

Table 10. Descriptive statistics of the power-line flicker in phase L1 at the tested measuring point.

Parameter	Period 1			Period 2		
	Cluster 1	Cluster 2	Cluster 3	Cluster 1	Cluster 2	Cluster 3
Min	0.0485	0.0465	0.0567	0.0399	0.0480	0.0518
1st Qu	0.1711	0.1508	0.1365	0.1755	0.1600	0.1506
Median	0.2712	0.2598	0.2316	0.2831	0.2665	0.2535
Mean	0.2680	0.2598	0.2434	0.2798	0.2634	0.2618
3rd Qu	0.3507	0.3479	0.3323	0.3676	0.3491	0.3533
Max	0.9148	1.2137	0.7278	1.1461	0.9753	1.6727
St. Dev.	0.1167	0.1258	0.1209	0.1256	0.1237	0.1400

Table 11. Descriptive statistics of the power-line flicker in phase L2 at the tested measuring point.

Parameter	Period 1			Period 2		
	Cluster 1	Cluster 2	Cluster 3	Cluster 1	Cluster 2	Cluster 3
Min	0.0495	0.0486	0.0566	0.0434	0.0499	0.0532
1st Qu	0.1746	0.1541	0.1434	0.1762	0.1610	0.1557
Median	0.2738	0.2621	0.2393	0.2859	0.2682	0.2550
Mean	0.2736	0.2631	0.2464	0.2817	0.2648	0.2647
3rd Qu	0.3540	0.3499	0.3334	0.3705	0.3506	0.3562
Max	1.8105	1.2550	0.7918	0.9101	1.4730	1.3985
St. Dev.	0.1250	0.1263	0.1187	0.1251	0.1270	0.1377

Table 12. Descriptive statistics of the power-line flicker in phase L3 at the tested measuring point.

Parameter	Period 1			Period 2		
	Cluster 1	Cluster 2	Cluster 3	Cluster 1	Cluster 2	Cluster 3
Min	0.0498	0.0480	0.0587	0.0416	0.0478	0.0515
1st Qu	0.1685	0.1499	0.1357	0.1746	0.1581	0.1533
Median	0.2770	0.2621	0.2375	0.2928	0.2687	0.2662
Mean	0.2717	0.2587	0.2435	0.2833	0.2659	0.2701
3rd Qu	0.3538	0.3462	0.3364	0.3738	0.3547	0.3617
Max	2.1364	1.2275	0.7420	1.4009	2.2206	2.1247
St. Dev.	0.1254	0.1239	0.1212	0.1275	0.1328	0.1587

The statistical tests and test hypotheses show that the power-line flickers did not change (red, Table 13) between Periods 1 and 2 for Cluster 1 (night) and Cluster 3 (generation covers demand). The power-line flickers varied between periods for Cluster 2 (generation with MG does not cover demand). The change in the P_{lt} between periods was not associated with a significant generation with MG. The results of the Wilcoxon rank-sum test are shown in Figure 10.

Phase | Period 1 | Period 2
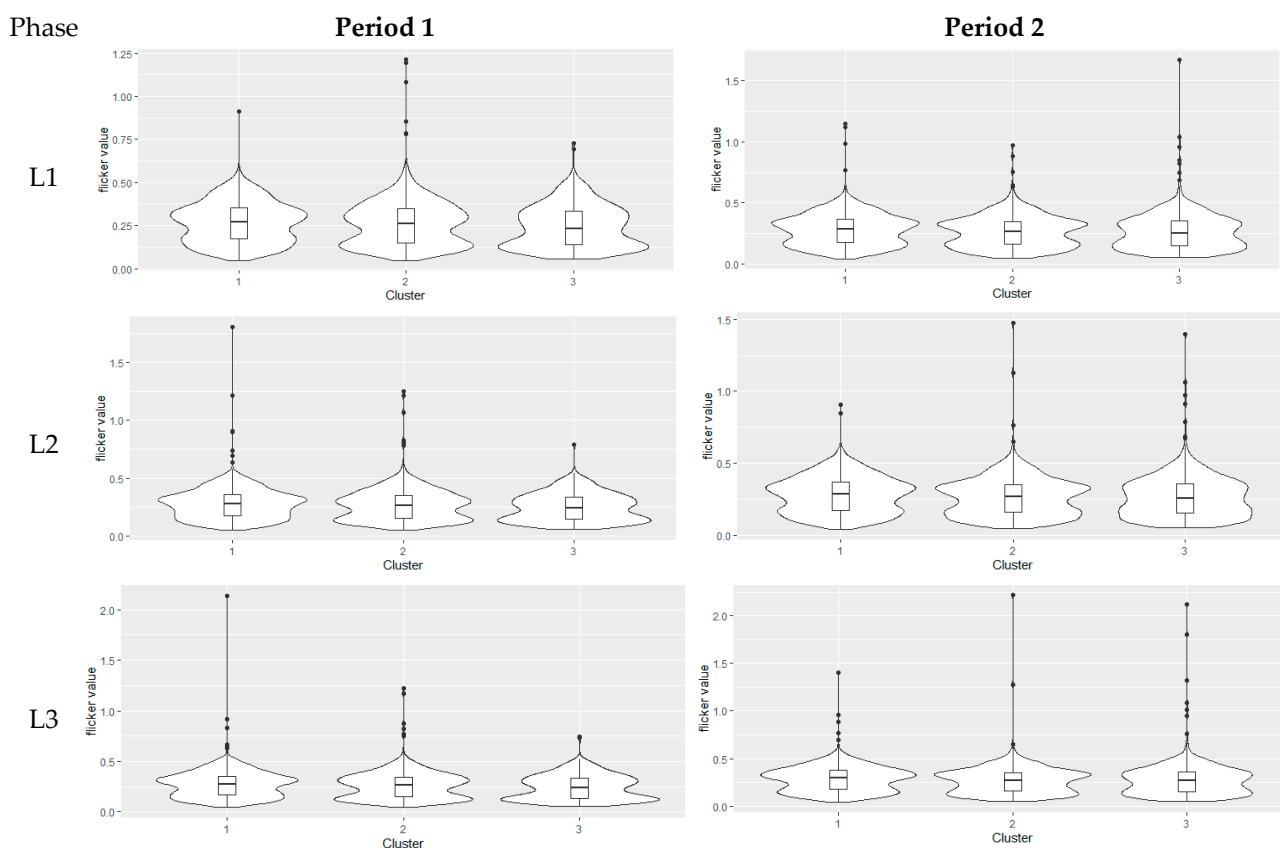
Figure 10. Violin plots of power-line flicker comparing clusters for Period 1 and Period 2 in each phase.

**Table 13.** Wilcoxon rank-sum test of the power-line flicker ($\alpha = 0.05$) in each phase.

Phase	Clusters	1	2	3
L1	W=	2,532,889	1,703,690	250,796
	p-value	0.00254	0.2521	0.02278
L2	W=	2,556,778	1,722,794	251,462
	p-value	0.01272	0.5712	0.02804
L3	W=	2,520,772	1,685,785	244,808
	p-value	0.001018	0.09141	0.002701

Data marked in red: the null hypothesis is true, which means values do not change between periods.

4.2.4. Voltage Unbalance Factor

Statistical tests were performed for the voltage unbalance factor k_{u2}. The data were statistically analyzed for each phase on the basis of the following values: minimum, maximum, mean, median, standard deviation, first and third quantiles (Table 14), confirming that the parameters were within the required range. The Wilcoxon rank-sum test was carried out with continuity correction for each phase (Table 15) on the significance level $\alpha = 0.05$. Null hypothesis: true location shift between the same clusters in different periods is 0 (red color in table). Alternative hypothesis: true location shift is not equal to 0 (black color in table). Data distribution is shown in the violin plots (Figure 11) and box plots (Figure 12) for both periods.

Table 14. Descriptive statistics of the voltage unbalance factor k_{u2} at the tested measuring point.

Parameter	Period 1			Period 2		
	Cluster 1	Cluster 2	Cluster 3	Cluster 1	Cluster 2	Cluster 3
Min	0.140	0.111	0.139	0.049	0.042	0.069
1st Qu	0.216	0.204	0.238	0.130	0.124	0.142
Median	0.247	0.241	0.274	0.152	0.148	0.171
Mean	0.249	0.247	0.275	0.152	0.148	0.172
3rd Qu	0.279	0.284	0.308	0.172	0.173	0.198
Max	0.386	0.425	0.435	0.248	0.263	0.307
St. Dev.	0.044	0.056	0.053	0.029	0.036	0.040

Table 15. Wilcoxon rank-sum test of the voltage unbalance factor k_{u2} ($\alpha = 0.05$).

Clusters	1	2	3
W=	5,205,856	3,276,778	507,850
p-value	$<2.2 \times 10^{-16}$	$<2.2 \times 10^{-16}$	$<2.2 \times 10^{-16}$

Data marked in red: the null hypothesis is true, which means values do not change between periods.
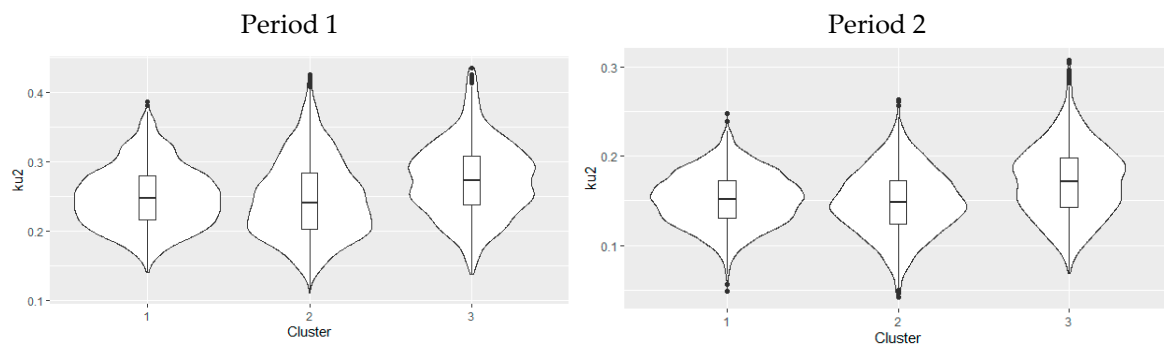
Figure 11. Violin plots of voltage unbalance factor k_{u2} comparing clusters for Period 1 and Period 2.
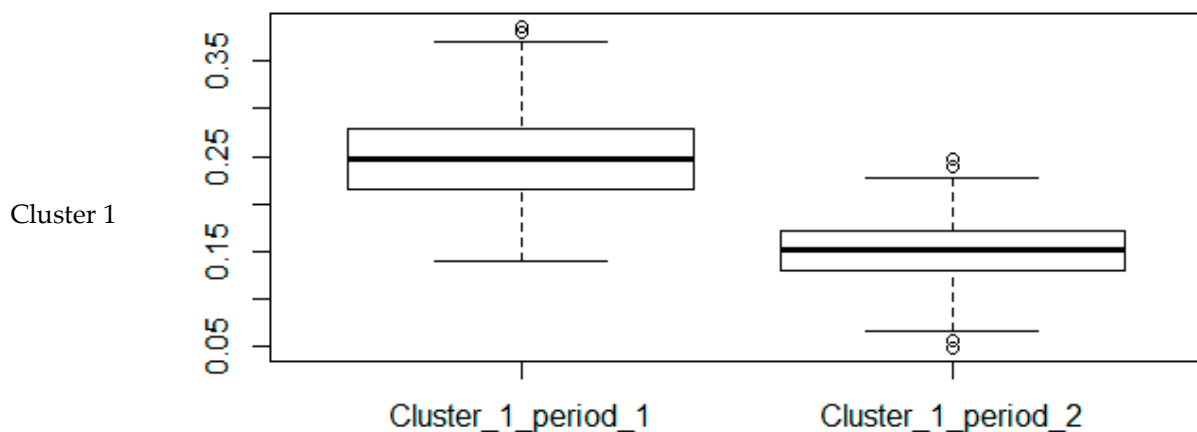

Figure 12. *Cont*.
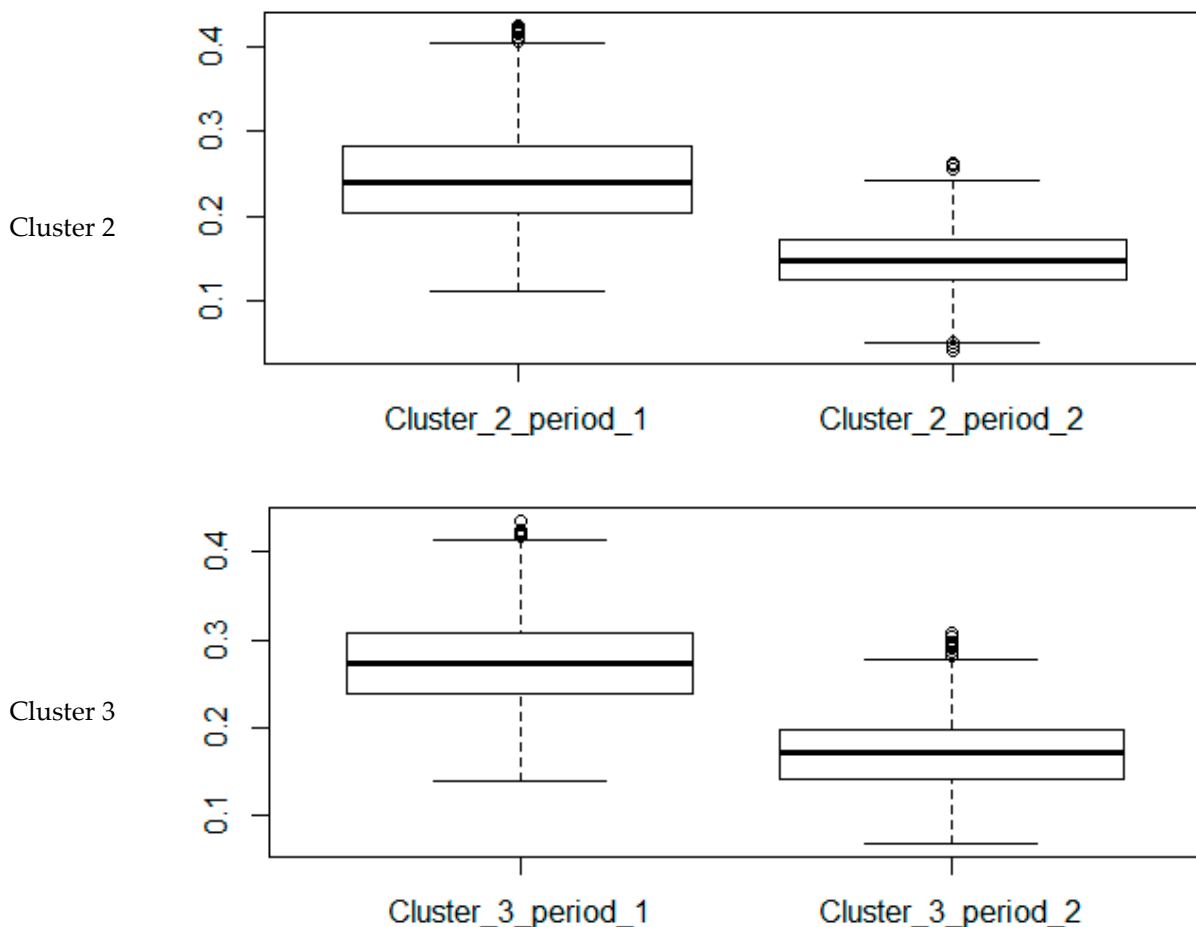
Figure 12. Box plots of voltage unbalance factor k_{u2} comparing periods for individual clusters in each phase.

The statistical tests and test hypotheses show that the voltage unbalance factor varied (red, Table 15) between Periods 1 and 2 for all clusters. The value of k_{u2} improved, and the value range approached zero. The change in the k_{u2} between periods was not associated with a significant generation with MG but with the seasonality of the power system operation. The results of the Wilcoxon rank-sum test are shown in Figures 11 and 12.

Additionally, due to the nature of the parameter k_{u2}, we wanted to check the probabilistic distribution of this parameter (Table 16). Since the coefficient was in (0,1) we checked the Beta(a,b) distribution of k_{u2}. Using maximum likelihood estimators, we estimated the parameters *a* and *b* for each cluster and period, presented in Table 17.

Table 16. One sample Kołmogorov–Smirnov test with an alternative hypothesis: two-sided ($\alpha = 0.05$).

Data	Period 1			Period 2		
	Cluster 1	Cluster 2	Cluster 3	Cluster 1	Cluster 2	Cluster 3
D	0.027513	0.035645	0.037319	0.036627	0.036395	0.043335
p-value	0.06366	0.01093	0.421	0.003702	0.0222	0.05234

Data marked in red: the null hypothesis is true, which means values do not change between periods.

We conclude that on the significance level 0.05 there is no reason to reject the hypothesis that the distribution of the k_{u2} in Cluster 1, Cluster 3 (Period 1) and Cluster 3 (Period 2) is beta with the shape parameters indicated above. In the other cases, we reject the null hypothesis.

Table 17. Estimated parameters for the beta distribution of k_{u2}.

Parameter	Period 1			Period 2		
	Cluster 1	Cluster 2	Cluster 3	Cluster 1	Cluster 2	Cluster 3
a = Shape1	24.01255	14.72601	19.16599	21.48934	13.36818	14.73362
b = Shape2	72.23202	44.91723	50.66585	119.99269	76.79445	71.17371

4.2.5. Total Harmonic Distortion

Statistical tests were performed for the total harmonic distortion for voltage (THDu). The data was statistically analyzed for each phase: L1, L2, and L3, on the basis of the following values: minimum, maximum, mean, median, standard deviation, first and third quantiles (Tables 18–20), confirming that the parameters were within the required range. The Wilcoxon rank-sum test was carried out with continuity correction for each phase (Table 21) on the significance level $\alpha = 0.05$. Null hypothesis: true location shift between the same clusters in different periods is 0 (red color in table). Alternative hypothesis: true location shift is not equal to 0 (black color in table). The data distribution is shown in the violin plots (Figure 13) for both periods.

Table 18. Descriptive statistics of the THDu in phase L1 at the tested measuring point.

Parameter	Period 1			Period 2		
	Cluster 1	Cluster 2	Cluster 3	Cluster 1	Cluster 2	Cluster 3
Min	0.9641	1.102	1.090	1.168	1.101	1.124
1st Qu	1.3802	1.336	1.326	1.535	1.392	1.391
Median	1.5236	1.446	1.388	1.672	1.477	1.447
Mean	1.5343	1.503	1.481	1.650	1.506	1.453
3rd Qu	1.6556	1.627	1.515	1.765	1.604	1.514
Max	2.2258	2.453	2.329	2.131	1.979	1.892
St. Dev.	0.2197	0.2378	0.2676	0.1534	0.1683	0.1051

Table 19. Descriptive statistics of the THDu in phase L2 at the tested measuring point.

Parameter	Period 1			Period 2		
	Cluster 1	Cluster 2	Cluster 3	Cluster 1	Cluster 2	Cluster 3
Min	1.059	1.108	1.139	1.267	1.220	1.244
1st Qu	1.438	1.379	1.331	1.599	1.455	1.470
Median	1.593	1.496	1.424	1.722	1.531	1.522
Mean	1.589	1.555	1.511	1.704	1.561	1.529
3rd Qu	1.721	1.685	1.558	1.809	1.665	1.580
Max	2.217	2.545	2.344	2.200	1.990	1.897
St. Dev.	0.2181	0.2441	0.2808	0.1503	0.1522	0.0937

Table 20. Descriptive statistics of the THDu in phase L3 at the tested measuring point.

Parameter	Period 1			Period 2		
	Cluster 1	Cluster 2	Cluster 3	Cluster 1	Cluster 2	Cluster 3
Min	0.9732	1.057	1.141	1.216	1.176	1.244
1st Qu	1.3760	1.353	1.339	1.507	1.422	1.470
Median	1.5356	1.486	1.411	1.654	1.526	1.522
Mean	1.5363	1.544	1.504	1.641	1.550	1.529
3rd Qu	1.6641	1.687	1.526	1.770	1.665	1.580
Max	2.1901	2.555	2.358	2.164	2.088	1.897

Table 21. Wilcoxon rank-sum test of the THDu ($\alpha = 0.05$) in each phase.

Phase	Clusters	1	2	3
L1	W =	1,668,852	1,584,933	219,530
	p-value	$<2.2 \times 10^{-16}$	2.086×10^{-06}	1.437×10^{-09}
L2	W =	1,715,456	1,538,138	174,365
	p-value	$<2.2 \times 10^{-16}$	7.122×10^{-10}	$<2.2 \times 10^{-16}$
L3	W =	1,846,383	1,571,882	160,227
	p-value	$<2.2 \times 10^{-16}$	2.739×10^{-07}	$<2.2 \times 10^{-16}$

Data marked in red: the null hypothesis is true, which means values do not change between periods.
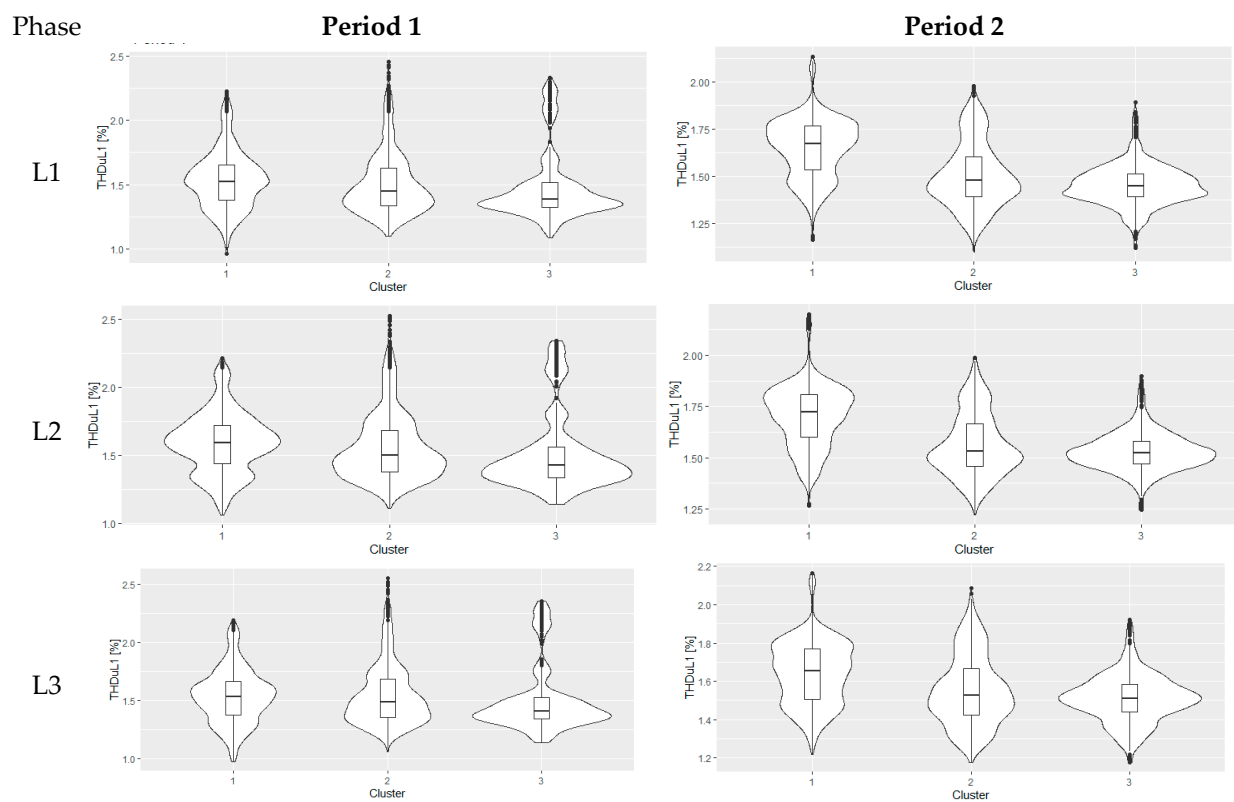
Figure 13. Violin plots of THDu comparing clusters for Period 1 and Period 2 in each phase.

The statistical tests and test hypotheses show that the THDu coefficient varies (red, Table 21) between Periods 1 and 2 for all clusters. The THDu coefficient improved in Period 2, especially for Cluster 3, which has a smaller maximum value, and a narrower value variation band and shifted closer to zero. The results of the Wilcoxon rank-sum test are shown in Figure 13.

5. Conclusions

Power quality in microgrids has become an up-to-date research element in smart grid and distribution power systems. Microgrids mainly contain different renewable energy sources, MG energy management system controllers and communication devices. The RESs, for example, photovoltaic plants, often use various technological developments, such as power electronics-based technologies. Thus, the structure of the microgrids can be a source of additional power quality problems. This paper assesses the impact of a microgrid implementation in a real distribution network on power quality indicators. The study includes a classical assessment of the long-term PQ parameters and statistical evaluation based on cluster analysis.

Compared to the period before the microgrid connection, the parameters influenced by the installation of the photovoltaic source is voltage and THDu. The installation connection does not affect the frequency and voltage unbalance factor values. K_{u2} and flickers are affected by the seasonality of the network operation.

The statistical tests indicate the seasonality of the data, which is related to the fact that the measurement periods were not conducted in the same months. It was influenced by the seasonal nature of the load and insolation. The clusters were divided manually, taking into account the periodicity of sources and loads during the day.

In further research, it is possible to establish another possibility of dividing the data based on the statistical properties of the data and using change point analysis methods. Note that in all analyses we included the outliers. They make up a large part of the observation. Subsequent analysis will be aimed at determining the nature of outliers in order to eliminate them from the analyses. Additionally, the examined facility allows for further tests in a new configuration of generation and receiving facilities, for other periods, or for checking the response of the network after adding additional sources such as wind and gas turbines.

As a future prospect, the obtained dataset can be used as input for the data mining process. This process may reveal specific working conditions which are also important from the point of view of the PQ assessment.

Author Contributions: Conceptualization, T.S.; data curation, A.O., Ł.M., M.S. and P.K.; formal analysis, A.O., Ł.M., M.S. and M.J.; funding acquisition, G.M. and T.R.; investigation, A.O., Ł.M., M.S., M.J. and T.S.; methodology, M.J.; project administration, T.S., R.L., G.M. and T.R.; resources, T.S., P.K., R.L., G.M. and T.R.; software, A.O., Ł.M. and M.S.; supervision, M.J. and T.S.; validation, M.S., M.J. and T.S.; visualization, A.O., Ł.M. and M.S.; writing—original draft, A.O., Ł.M. and M.S.; writing—review and editing, M.J. and T.S. All authors have read and agreed to the published version of the manuscript.

Data Availability Statement: Data will be sent on request to the corresponding author.

Conflicts of Interest: The authors declare no conflict of interest.

Abbreviations

Qu	quantiles (successively 1st, 2nd, 3rd, 4th)
A	Anderson–Darling normality
AC	alternating current
D	Kołmogorov–Smirnov test
DC	direct current
DER	distributed energy resources
DG	distributed generation
ESS	energy storage system
f	power frequency
GPQI	global power quality index
ILC	bidirectional interlinking converter
IQR	interquartile range
ku2	voltage unbalance factor
LV	low voltage
max	maximum value
MG	microgrid
min	minimum value
MV	middle voltage
MW	mega watt (coherent unit of power)
PCC	point of common coupling
P_{lt}	flicker severity
PQ	power quality
PQI	power quality indices
PV	photovoltaic, photovoltaic power unit
p-value	rank-sum test statistic W
PVDG	photovoltaic distributed generation
RES	renewable energy sources
RMS	root-mean-square value
SPWM	sinusoidal pulse width modulation
St. Dev.	standard deviation
TDD	total demand distortion
THC	total harmonic current
THD	total harmonic distortion
THDu	total harmonic distortion for voltage
$THDu_{L1}$, $THDu_{L2}$, $THDu_{L3}$	total harmonic distortion for voltage in each phase: L1, L2, L3
U	voltage
U_{L1}, U_{L2}, U_{L3}	phase voltage in phase: L1, L2, L3
W	test statistic value

References

1. Levenda, A.M.; Behrsin, I.; Disano, F. Renewable Energy for Whom? A Global Systematic Review of the Environmental Justice Implications of Renewable Energy Technologies. *Energy Res. Soc. Sci.* **2021**, *71*, 101837.
2. Li, L.; Lin, J.; Wu, N.; Xie, S.; Meng, C.; Zheng, Y.; Wang, X.; Zhao, Y. Review and Outlook on the International Renewable Energy Development. *Energy Built Environ.* **2022**, *3*, 139–157. [CrossRef]
3. Maradin, D. Advantages and Disadvantages of Renewable Energy Sources Utilization. *Int. J. Energy Econ. Policy* **2021**, *11*, 176–183. [CrossRef]
4. Radmehr, R.; Shayanmehr, S.; Ali, E.B.; Ofori, E.K.; Jasińska, E.; Jasiński, M. Exploring the Nexus of Renewable Energy, Ecological Footprint, and Economic Growth through Globalization and Human Capital in G7 Economics. *Sustainability* **2022**, *14*, 12227. [CrossRef]
5. Hernik, J.; Noszczyk, T.; Rutkowska, A. Towards a Better Understanding of the Variables That Influence Renewable Energy Sources in Eastern Poland. *J. Clean. Prod.* **2019**, *241*, 118075. [CrossRef]
6. Szyba, M. Spatial Planning and the Development of Renewable Energy Sources in Poland. *Acta Innov.* **2021**, *2021*, 5–14. [CrossRef]
7. Paska, J.; Surma, T.; Terlikowski, P.; Zagrajek, K. Electricity Generation from Renewable Energy Sources in Poland as a Part of Commitment to the Polish and EU Energy Policy. *Energies* **2020**, *13*, 4261. [CrossRef]

8. Ahmed, N.; Sheikh, A.A.; Mahboob, F.; Ali, M.S.; Jasińska, E.; Jasiński, M.; Leonowicz, Z.; Burgio, A. Energy Diversification: A Friend or Foe to Economic Growth in Nordic Countries? A Novel Energy Diversification Approach. *Energies* **2022**, *15*, 5422. [CrossRef]

9. Hatziargyriou, N. *Microgrids: Architectures and Control*; John Wiley & Sons: Hoboken, NJ, USA, 2013.

10. Gust, G.; Brandt, T.; Mashayekh, S.; Heleno, M.; DeForest, N.; Stadler, M.; Neumann, D. Strategies for Microgrid Operation under Real-World Conditions. *Eur. J. Oper. Res.* **2021**, *292*, 339–352. [CrossRef]

11. Ghorbanian, M.; Dolatabadi, S.H.; Siano, P. Big Data Issues in Smart Grids: A Survey. *IEEE Syst. J.* **2019**, *13*, 4158–4168. [CrossRef]

12. Dhupia, B.; Usha Rani, M.; Alameen, A. The Role of Big Data Analytics in Smart Grid Management. In *Emerging Research in Data Engineering Systems and Computer Communications*; Springer: Berlin/Heidelberg, Germany, 2020; Volume 1054, pp. 403–412.

13. Golla, M.; Sankar, S.; Chandrasekaran, K. Renewable Integrated UAPF Fed Microgrid System for Power Quality Enhancement and Effective Power Flow Management. *Int. J. Electr. Power Energy Syst.* **2021**, *133*, 107301. [CrossRef]

14. Ding, Y. Analysis of Operation and Maintenance of Power Distribution Network Management Technology under the Background of Big Data Era. In *Advances in Intelligent Systems and Computing*; Springer: Berlin/Heidelberg, Germany, 2020; Volume 1117.

15. Jasiński, M.; Sikorski, T.; Borkowski, K. Clustering as a Tool to Support the Assessment of Power Quality in Electrical Power Networks with Distributed Generation in the Mining Industry. *Electr. Power Syst. Res.* **2019**, *166*, 52–60. [CrossRef]

16. Nair, D.R.; Nair, M.G.; Thakur, T. A Smart Microgrid System with Artificial Intelligence for Power-Sharing and Power Quality Improvement. *Energies* **2022**, *15*, 5409. [CrossRef]

17. Guo, X.-H.; Chang, C.-W.; Chang-Chien, L.-R. Digital Implementation of Harmonic and Unbalanced Load Compensation for Voltage Source Inverter to Operate in Grid Forming Microgrid. *Electronics* **2022**, *11*, 886. [CrossRef]

18. Moreno Escobar, J.J.; Morales Matamoros, O.; Tejeida Padilla, R.; Lina Reyes, I.; Quintana Espinosa, H. A Comprehensive Review on Smart Grids: Challenges and Opportunities. *Sensors* **2021**, *21*, 6978. [PubMed]

19. Jasiński, M. Combined Correlation and Cluster Analysis for Long-Term Power Quality Data from Virtual Power Plant. *Electronics* **2021**, *10*, 641. [CrossRef]

20. Jasinski, M.; Martirano, L.; Najafi, A.; Homaee, O.; Leonowicz, Z.; Kermani, M. Microgrid Working Conditions Identification Based on Cluster Analysis—A Case Study From Lambda Microgrid. *IEEE Access* **2022**, *10*, 70971–70979. [CrossRef]

21. Choudhury, S. Review of Energy Storage System Technologies Integration to Microgrid: Types, Control Strategies, Issues, and Future Prospects. *J. Energy Storage* **2022**, *48*, 103966. [CrossRef]

22. Tembo, G. Overview of the Microgrid Concept and Its Hierarchical Control Architecture. *Int. J. Eng. Res. Technol.* **2016**, *5*, 1–6.

23. Marchand, S.; Monsalve, C.; Reimann, T.; Heckmann, W.; Ungerland, J.; Lauer, H.; Ruhe, S.; Krauß, C. Microgrid Systems: Towards a Technical Performance Assessment Frame. *Energies* **2021**, *14*, 2161. [CrossRef]

24. Zia, M.F.; Elbouchikhi, E.; Benbouzid, M. Microgrids Energy Management Systems: A Critical Review on Methods, Solutions, and Prospects. *Appl. Energy* **2018**, *222*, 1033–1055. [CrossRef]

25. Vanashi, H.K.; Mohammadi, F.D.; Verma, V.; Solanki, J.; Solanki, S.K. Hierarchical Multi-Agent Based Frequency and Voltage Control for a Microgrid Power System. *Int. J. Electr. Power Energy Syst.* **2022**, *135*, 107535. [CrossRef]

26. Yoldaş, Y.; Önen, A.; Muyeen, S.M.; Vasilakos, A.V.; Alan, İ. Enhancing Smart Grid with Microgrids: Challenges and Opportunities. *Renew. Sustain. Energy Rev.* **2017**, *72*, 205–214. [CrossRef]

27. Nasser, N.; Fazeli, M. Buffered-Microgrid Structure for Future Power Networks; A Seamless Microgrid Control. *IEEE Trans. Smart Grid* **2021**, *12*, 131–140. [CrossRef]

28. Zhou, Y.; Ngai-Man Ho, C. A Review on Microgrid Architectures and Control Methods. In Proceedings of the 2016 IEEE 8th International Power Electronics and Motion Control Conference, IPEMC-ECCE Asia 2016, Hefei, China, 22–26 May 2016.

29. Rajesh, K.S.; Dash, S.S.; Rajagopal, R.; Sridhar, R. A Review on Control of Ac Microgrid. *Renew. Sustain. Energy Rev.* **2017**, *71*, 814–819. [CrossRef]

30. Sarangi, S.; Sahu, B.K.; Rout, P.K. Review of Distributed Generator Integrated AC Microgrid Protection: Issues, Strategies, and Future Trends. *Int. J. Energy Res.* **2021**, *45*, 14117–14144. [CrossRef]

31. Al-Ismail, F.S. DC Microgrid Planning, Operation, and Control: A Comprehensive Review. *IEEE Access* **2021**, *9*, 36154–36172. [CrossRef]

32. Chandra, A.; Singh, G.K.; Pant, V. Protection Techniques for DC Microgrid—A Review. *Electr. Power Syst. Res.* **2020**, *187*, 106439. [CrossRef]

33. Mariscotti, A. Power Quality Phenomena, Standards, and Proposed Metrics for DC Grids. *Energies* **2021**, *14*, 6453. [CrossRef]

34. Sahoo, S.K.; Sinha, A.K.; Kishore, N.K. Control Techniques in AC, DC, and Hybrid AC-DC Microgrid: A Review. *IEEE J. Emerg. Sel. Top. Power Electron.* **2018**, *6*, 738–759. [CrossRef]

35. Ahmed, M.; Meegahapola, L.; Vahidnia, A.; Datta, M. Stability and Control Aspects of Microgrid Architectures-A Comprehensive Review. *IEEE Access* **2020**, *8*, 144730–144766. [CrossRef]

36. Patrao, I.; Figueres, E.; Garcerá, G.; González-Medina, R. Microgrid Architectures for Low Voltage Distributed Generation. *Renew. Sustain. Energy* **2015**, *43*, 415–424. [CrossRef]

37. Sahoo, B.; Routray, S.K.; Rout, P.K. AC, DC, and Hybrid Control Strategies for Smart Microgrid Application: A Review. *Int. Trans. Electr. Energy Syst.* **2021**, *31*, e12683. [CrossRef]

38. Astriani, Y.; Shafiullah, G.M.; Anda, M.; Hilal, H. Techno-Economic Evaluation of Utilizing a Small-Scale Microgrid. *Energy Procedia* **2019**, *158*, 3131–3137. [CrossRef]

39. Chandak, S.; Rout, P.K. The Implementation Framework of a Microgrid: A Review. *Int. J. Energy Res.* **2021**, *45*, 3523–3547. [CrossRef]

40. Alayi, R.; Zishan, F.; Mohkam, M.; Hoseinzadeh, S.; Memon, S.; Garcia, D.A. A Sustainable Energy Distribution Configuration for Microgrids Integrated to the National Grid Using Back-to-Back Converters in a Renewable Power System. *Electronics* **2021**, *10*, 1826. [CrossRef]

41. Iweh, C.D.; Gyamfi, S.; Tanyi, E.; Effah-Donyina, E. Distributed Generation and Renewable Energy Integration into the Grid: Prerequisites, Push Factors, Practical Options, Issues and Merits. *Energies* **2021**, *14*, 5375. [CrossRef]

42. Chen, S.; Zhang, J.; Wang, L.; Zhang, H.; Li, L. Evaluation of Power Quality and Reliability of Distributed Generation in Smart Grid. In Proceedings of the IOP Conference Series: Earth and Environmental Science, Jakarta, Indonesia, 25–26 September 2021; Volume 632.

43. Dragicevic, T.; Vazquez, S.; Wheeler, P. Advanced Control Methods for Power Converters in Distributed Generation Systems and Microgrids. *IEEE Trans. Ind. Electron.* **2019**, *66*, 8866–8869. [CrossRef]

44. Martirano, L.; Jasinski, M.; Najafi, A.; Cocira, V.; Leonowicz, Z. Integration of Supervision and Monitoring Systems of Microgrids— A Case Study from Lambda Microgrid for Correlation Analysis. In Proceedings of the 2021 IEEE International Conference on Environment and Electrical Engineering and 2021 IEEE Industrial and Commercial Power Systems Europe (EEEIC/I&CPS Europe), Bari, Italy, 7–10 September 2021; pp. 1–4.

45. Liao, J.; Zhou, N.; Wang, Q.; Li, C.; Yang, J. Definition and Correlation Analysis of Power Quality Index of DC Distribution Network. *Zhongguo Dianji Gongcheng Xuebao/Proc. Chin. Soc. Electr. Eng.* **2018**, *38*, 6847–6860. [CrossRef]

46. Silva, E.N.M.; Rodrigues, A.B.; da Guia Da Silva, M. Stochastic Assessment of the Impact of Photovoltaic Distributed Generation on the Power Quality Indices of Distribution Networks. *Electr. Power Syst. Res.* **2016**, *135*, 59–67. [CrossRef]

47. Shi, H.; Zhuo, F.; Yi, H.; Geng, Z. Control Strategy for Microgrid under Three-Phase Unbalance Condition. *J. Mod. Power Syst. Clean Energy* **2016**, *4*, 94–102. [CrossRef]

48. Liu, B.; Zhao, X.; Liu, Y.; Zhu, Y.; Chen, J. Control Strategy of Clustered Micro-Grids for Grid Voltage Unbalance Compensation without Communications. *IET Gener. Transm. Distrib.* **2020**, *14*, 4410–4415. [CrossRef]

49. Arbab-Zavar, B.; Palacios-Garcia, E.J.; Vasquez, J.C.; Guerrero, J.M. Smart Inverters for Microgrid Applications: A Review. *Energies* **2019**, *12*, 840. [CrossRef]

50. Golkhandan, N.H.; Ali Chamanian, M.; Tahami, F. A New Control Method for Elimination of Current THD under Extremely Polluted Grid Conditions Applied on a Three Phase PWM Rectifier. In Proceedings of the INTELEC, International Telecommunications Energy Conference (Proceedings), Turino, Italy, 7–11 October 2018.

51. Li, G.; Zhang, X. Comparison between Two Probabilistic Load Flow Methods for Reliability Assessment. In Proceedings of the 2009 IEEE Power Energy Society General Meeting, Calgary, AB, Canada, 26–30 July 2009; pp. 1–7.

52. Li, Y.; Nejabatkhah, F. Overview of Control, Integration and Energy Management of Microgrids. *J. Mod. Power Syst. Clean Energy* **2014**, *2*, 212–222. [CrossRef]

53. Sakar, S.; Balci, M.E.; Abdel Aleem, S.H.E.; Zobaa, A.F. Integration of Large-Scale PV Plants in Non-Sinusoidal Environments: Considerations on Hosting Capacity and Harmonic Distortion Limits. *Renew. Sustain. Energy Rev.* **2018**, *82*, 176–186.

54. Zhang, M.; Li, Y.; Liu, F.; Li, W.; Peng, Y.; Wu, W.; Cao, Y. Cooperative Operation of DG Inverters and a RIHAF for Power Quality Improvement in an Integrated Transformer-Structured Grid-Connected Microgrid. *IEEE Trans. Ind. Appl.* **2019**, *55*, 1157–1170. [CrossRef]

55. Pourarab, M.; Meyer, J.; Stiegler, R. Assessment of Harmonic Contribution of a Photovoltaic Installation Based on Field Measurements. *Renew. Energy Power Qual. J.* **2017**, *1*, 865–870. [CrossRef]

56. Wang, N.; Zheng, S.; Gao, W. Microgrid Harmonic Mitigation Strategy Based on the Optimal Allocation of Active Power and Harmonic Mitigation Capacities of Multi-Functional Grid-Connected Inverters. *Energies* **2022**, *15*, 6109. [CrossRef]

57. Michalec, Ł.; Jasiński, M.; Sikorski, T.; Leonowicz, Z.; Jasiński, Ł.; Suresh, V. Impact of Harmonic Currents of Nonlinear Loads on Power Quality of a Low Voltage Network—Review and Case Study. *Energies* **2021**, *14*, 3665. [CrossRef]

58. Javadi, M.; Gong, Y.; Chung, C.Y. Frequency Stability Constrained Microgrid Scheduling Considering Seamless Islanding. *IEEE Trans. Power Syst.* **2022**, *37*, 306–316. [CrossRef]

59. Iqbal, A.; Ayoub, A.; Waqar, A.; Ul-Haq, A.; Zahid, M.; Haider, S. Voltage Stability Enhancement in Grid-Connected Microgrid Using Enhanced Dynamic Voltage Restorer (EDVR). *AIMS Energy* **2021**, *9*, 150–177. [CrossRef]

60. Ortega, R.; García, V.H.; García-García, A.L.; Rodriguez, J.J.; Vásquez, V.; Sosa-Savedra, J.C. Modeling and Application of Controllers for a Photovoltaic Inverter for Operation in a Microgrid. *Sustainability* **2021**, *13*, 5115. [CrossRef]

61. Howlader, A.M.; Sadoyama, S.; Roose, L.R.; Chen, Y. Active Power Control to Mitigate Voltage and Frequency Deviations for the Smart Grid Using Smart PV Inverters. *Appl. Energy* **2020**, *258*, 114000. [CrossRef]

62. Liu, Z.; Xu, X.; Abdelsalam, H.A.; Makram, E. Power System Harmonics Study for Unbalanced Microgrid System with PV Sources and Nonlinear Loads. *J. Power Energy Eng.* **2015**, *3*, 43–55. [CrossRef]

63. Sun, X.; Lei, W.; Dai, Y.; Yin, Y.; Liu, Q. Optimization Configuration of Grid-Connected Inverters to Suppress Harmonic Amplification in a Microgrid. *Energies* **2022**, *15*, 4989. [CrossRef]

64. *IEEE Std 519-2014 (Revision of IEEE Std 519-1992)*; IEEE Recommended Practice and Requirements for Harmonic Control in Electric Power Systems. IEEE: Piscataway, NJ, USA, 2014; Volume 2014.

65. Homaee, O.; Najafi, A.; Jasinski, M.; Tsaousoglou, G.; Leonowicz, Z. Coordination of Neighboring Active Distribution Networks under Electricity Price Uncertainty Using Distributed Robust Bi-Level Programming. *IEEE Trans. Sustain. Energy* **2022**, preonline. [CrossRef]
66. *EN 50160*; Voltage Characteristics of Electricity Supplied by Public Distribution Network. Orgalim: Brussels, Belgium, 2015.
67. Jasinski, M.; Sikorski, T.; Kaczorowska, D.; Kostyla, P.; Leonowicz, Z.; Rezmer, J.; Janik, P.; Bejmert, D. Global Power Quality Index Application in Virtual Power Plant. In Proceedings of the 2020 12th International Conference and Exhibition on Electrical Power Quality and Utilisation-(EPQU), Cracow, Poland, 14–15 September 2020; pp. 1–6.
68. *European Standard EN61000-4-30*; Electromagnetic Compatibility (EMC)—Part 4–30: Testing and Measurement Techniques—Power Quality Measurement Methods. International Electrotechnical Commission: Geneva, Switzerland, 2015.